High-order harmonics and isolated-attosecond pulse generation of Three-Dimensional H atom by UV-assisted chirped fields

Hong-Dan Zhang[1], Jing Guo[1,2,*], Hui-Ying Zhong[1], Xiang-Yi Luo[1,3], Hui Du[1], Yan Shi[1], Xuri Huang[2] and Xue-Shen Liu[1]

[1] *Institute of Atomic and Molecular Physics, Jilin University, Changchun 130012, China*
[2] *Institute of theoretical chemistry, Jilin University, Changchun 130012, China*
[3] *College of Physics, Baicheng Normal University, Baicheng 137000, China*

Abstract. By solving the time-dependent Schrödinger equation (TDSE) accurately with time-dependent generalized pseudospectral (TDGPS) method, we theoretically investigated the high-order-harmonic generation (HHG) from three dimensional (3D) Hydrogen atom in ultraviolet (UV)-assisted chirped fields. When a 128 nm UV pulse is added on a chirped fundamental field, the HHG spectra is greatly broadened and enhanced, which is quite similar as the HHG from H atom initially prepared in the first excited state in the chirped field only. Besides, the HHG of H atom in the combination of a chirped fundamental field and a 256 nm UV pulse case is also investigated. The HHG process is illustrated by the semi-classical three-step model and the time-frequency analysis. The ionization probability and electron wavepacket as functions of time are also calculated to further illustrate this phenomenon. Furthermore, we also discuss the influence of time delay between the chirped fundamental field and the 128 nm UV pulse on HHG process. Finally, by superposing the harmonics in the range of 200th-260th order, an isolated attosecond pulse with a duration of about 64 as can be generated.

PACS: 32.80.Rm, 42.65.Re, 42.65.Ky

Key words: High-order harmonic generation, generalized pseudospectral method, UV-assisted chirped fields, attosecond pulse

1 Introduction

With the development of laser technique, the ultrafast electron dynamics of atoms and molecules leads to a series of nonlinear nonperturbative phenomena, and attracts much

---

Corresponding author. Email address: `gjing@jlu.edu.cn` (J. Guo)

interest in ultrafast science and technology [1, 2, 3]. In particular, high-order harmonic generation (HHG), which occurs during the process of laser pulses interact with atoms or molecules, has been studied for more than two decades [4, 5, 6]. It is still a rapid growing field because of its potential to generate coherent light sources in ultraviolet to extreme ultraviolet (XUV) range and generating attosecond pulse. The HHG process can be well understood by the well-known semi-classical three-step model [7, 8, 9]: an electron first tunnels out of a Coulomb potential barrier suppressed by the field and moves away from the parent ion; then the freed-electron is pulled back and accelerated when the laser field direction is reversed; finally it recombines with the parent ion and emits a harmonic photon. In the past few years, many efforts have been paid to broaden the bandwidth of HHG by controlling the ionization process, including the employment of high-energy IR field [10, 11], multicolor fields [12, 13, 14, 15], Terahertz (THz) field [16, 17], static field [18, 19], the macroscopic propagation effect [20, 21], spatially inhomogeneous field [22, 23, 24] and chirped field [25, 26]. Generally, the intensity of HHG is decreased by using chirped laser pulse. Furthermore, many methods have been investigated to enhance intensity of HHG, including the coherent superposition of ground state and excited states in atoms [27, 28], adding an ultraviolet (UV) pulse [29, 30], or a noise field [31], and the two-cell harmonic generation effect [32]. Due to the high energy of photons, a UV pulse can facilitate the electronic transition of ground state [33, 34], and naturally acts as a trigger to increase the contributions of special electron paths [35, 36, 37]. Recently, Li *et al.* [38] have presented an efficient method to generate an ultrashort isolated 26 as pulse. Feng *et al.* [39] theoretically achieved an isolated 40 as pulse of He atom by means of the combination of a two-color chirped pulse and an ultrashort ultraviolet pulse.

In this paper, we investigate the extension and enhancement of HHG from three dimensional (3D) H atom in UV-assisted chirped fields by solving time-dependent Schrödinger equation (TDSE) accurately with time-dependent generalized pseudospectral (TDGPS) [40, 41] method. The corresponding time-frequency and three-step model are also presented to explain the difference between the chirped field only case and the combination of chirped fundamental field and a 128 nm UV pulse case. We also demonstrate the ionization probability and electron wavepacket as functions of time to further illustrate this phenomenon.

2 Model

In this paper, the interaction between laser pulse and H atom can be obtained by numerically solving 3D TDSE in spherical coordinates ($x = r\sin\theta\cos\varphi$, $y = r\sin\theta\sin\varphi$, and $z = r\cos\theta$), and the laser field is linearly polarized along the z axis. The 3D TDSE is given by (in atomic units (a.u.)):

$$i\frac{\partial \psi(r,t)}{\partial t} = \hat{H}\psi(r,t) = [\hat{H}_0 + \hat{V}(r,t)]\psi(r,t). \tag{1}$$

Here, $\hat{H}_0$ is the unperturbed Hamiltonian of H atom and V is the Coulomb potential

between H atom and an intense laser field,

$$\hat{H}_0 = -\frac{1}{2}\frac{d^2}{dr^2} + \frac{\hat{L}^2}{2r^2} - \frac{1}{r} \tag{2}$$

$$\hat{V}(r,t) = -E \cdot r = -E(z,t)z \tag{3}$$

where, $-\frac{1}{2}\frac{d^2}{dr^2}$ is radial kinetic energy, $\frac{\hat{L}^2}{2r^2}$ is centrifugal potential energy and $-\frac{1}{r}$ is atomic potential of H atom.

The TDSE is solved accurately and efficiently by means of the TDGPS. The numerical scheme of the TDGPS method allows for denser grids near the origin, leading to more accurate and efficient time propagation of the wavefunction with the use of a considerably smaller number of grid points than those of the equal-spacing grid methods. A second-order split-operator technique in the energy representation, which is different from the traditional split-operator technique, is used for the efficient and accurate time propagation of the wave function as follows:

$$\psi(r,t+\Delta t) = e^{-i\hat{H}_0\frac{\Delta t}{2}}e^{-i\hat{V}(r,\theta,t+\frac{\Delta t}{2})}e^{-i\hat{H}_0\frac{\Delta t}{2}}\psi(r,t) + O(\Delta t^3). \tag{4}$$

Once the time-dependent wave function is determined, then we can compute the expectation value of the induced dipole moment in the acceleration form:

$$\begin{aligned}d_A(t) &= \left\langle \psi(r,t) \left| \frac{\partial^2 z}{\partial t^2} \right| \psi(r,t) \right\rangle \\ &= \langle \psi(r,t) | [\hat{H},[\hat{H},z]] | \psi(r,t) \rangle.\end{aligned} \tag{5}$$

The corresponding HHG power spectrum can be obtained by Fourier transformation of the time-dependent dipole moments

$$P_A = (\omega) = \left| \frac{1}{t_f - t_i}\frac{1}{\omega^2}\int_{t_i}^{t_f} d_A(t)e^{-i\omega t} \right| \tag{6}$$

where t_i and t_f are the instants which control pulse turned on and off, respectively. The time-dependent electron wave packet distributions can be calculated by following equation:

$$G(r,t) = |\psi(r,t)|^2. \tag{7}$$

The electron ionization probability is obtained by

$$P_i(t) = 1 - \sum_{bound} |\langle \varphi_n(r) | \psi(r,t) \rangle dt|^2. \tag{8}$$

where the summation is over all the bound states $\varphi_n(r)$ when the field has been turned off.

The attosecond pulse can be calculated without any phase compensation by super-posing several harmonics as follows:

$$I(t) = \left| \sum_q a_q e^{iq\omega t} \right|^2.$$

$$(9)$$

where $a_q = \int d_A(t) e^{-i\omega t} dt$, q is harmonic order number. To study the detailed spectral and temporal structures of HHG, we perform time-frequency analysis by means of the wavelet transform,

$$A(t_0, \omega) = \int_{-\infty}^{\infty} f(t) w_{t_0, \omega}(t) dt$$

$$(10)$$

where $w_{t_0, \omega}(t)$ is the wavelet transform kernel, which can be shown as follows:

$$w_{t_0, \omega}(t) = \sqrt{\omega} W(w(t - t_0)).$$

$$(11)$$

where $W(x) = (1/\sqrt{\tau_0}) e^{ix} e^{-x^2/2\tau_0^2}$ is the Morlet wavelet.

3   Numerical results

In our calculation, we choose a chirped fundamental field only and the combination of the chirped fundamental field and a UV pulse, which can be expressed as follows:

$$E_0(t) = E_1 f_1(t) \cos(\omega_1 t + \delta(t))$$

$$(12)$$

$$E(t) = E_0(t) + E_i f_i(t - \tau) \cos(\omega_i(t - \tau))$$

$$(13)$$

where i=2,3, E_1=0.07549 a.u., E_2=E_3=0.007549 a.u. are the electric-field amplitudes, $f_1(t)$, $f_2(t-\tau)$, $f_3(t-\tau)$ are the Gaussian envelopes and the corresponding full width at half maximum (FWHM) are 5 fs, 2 fs and 2 fs, respectively. ω_1=0.038 a.u. (1200nm), ω_2=0.178 a.u. (256nm) and ω_3=0.356 a.u. (128nm) are the laser frequencies. The delay of the UV pulse and chirped fundamental field is defined as τ=-αT_0, where is the parameter of time delay, T_0=$2\pi/\omega_1$, $\delta(t)$=-$\beta\omega t^2/T$ presents the chirped fundamental field, where T=$10T_0$. The chirp form can be controlled by adjusting the parameter β. When $\beta = 0$, the pulse is chirp-free. Fig. 1(a) shows the time evolution of a chirp-free field only, a chirped field only, a 128 nm UV pulse only and a chirped fundamental field combined with a 128 nm UV pulse. The inset view shows a 256 nm UV pulse only and a chirped fundamental field combined with a 256 nm UV pulse as functions of time. From Fig. 1(a) we can see two different parameters of UV pulses are synthesized with a chirped fundamental field at -0.5 O.C. (O.C. denotes optical cycle), respectively, then the combined laser field has a small tremor. Fig. 1(b) presents the HHG for the chirp-free field only case, which has a double-plateau structure with two cutoffs of the 63th order and 96th order. For the chirped field only case, it can apparently be seen that the first plateau is extended to about 120th order, the intensity of the first plateau is approximately two orders lower than that
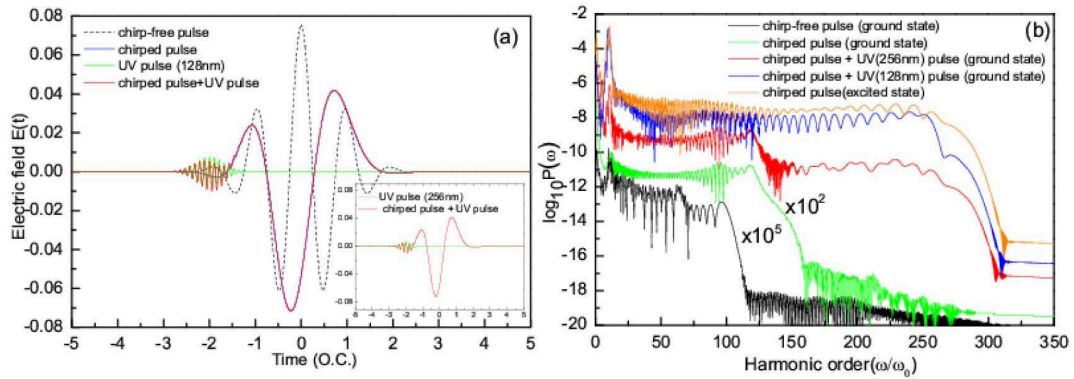
Figure 1: (Color online) (a) A chirp-free fundamental field only ($\beta = 0$, black dotted curve), a chirped fundamental field only with $\beta = 0.55$ (blue solid curve), a 128 nm UV field only with $\alpha = 2.0$ (green solid curve) and a chirped fundamental field combined with a 128 nm UV field (red solid curve). A inset view of a 256 nm UV field only with $\alpha = 2.0$ (green solid curve) and a chirped fundamental field combined with a 256 nm UV field (red solid curve). (b) The corresponding HHG from H atom initially prepared in the ground state in the chirp-free fundamental field only (black solid curve), the chirped fundamental field only (green solid curve), the chirped fundamental field combined with a 256 nm UV field (red solid curve), the chirped fundamental field combined with a 128 nm UV field (blue solid curve). The corresponding HHG from H atom initially prepared in the excited state in the chirped fundamental field only (orange solid curve).

of chirp-free field only case. Whereas in the chirped fundamental field combined with a 256 nm UV pulse case, the harmonic spectrum presents a double-plateau structure with two cutoffs of 120th order and 260th order, the intensity of the second plateau is about six orders higher than that of chirped field only case. Besides, the second plateau is continuous, a broadband supercontinuum with a 145-eV bandwidth can be clearly seen. When we use a 128 nm UV pulse instead of the 256 nm UV pulse, surprisingly, the two plateaus merge into one plateau and a broadband supercontinuum can be achieved.

Furthermore, the intensity of HHG in the combination of a chirped fundamental field and a 128 nm UV pulse case is about three orders higher than that in the combination of a chirped fundamental field and a 256 nm UV pulse case, this is because its photon energy of E_{128nm} = 10.3 eV is close to that of the one-photon transition between the ground and 1st excited states of the H atom. As a result, the electron can be easily excited to 1st excited state and then further ionized by the laser field. We also investigate the corresponding HHG from H atom initially prepared in the 1st excited state in the chirped fundamental field only, which is also shown in Fig. 1(b) and the result shows the HHG is almost the same as that of HHG from H atom initially prepared in the ground state in the combination of a chirped fundamental field and a 128 nm UV pulse case. Indeed, this is the main physical mechanism behind the harmonic enhancement by this combination scheme.

In order to better understand the physical mechanism of HHG, we investigate the time-frequency profile of the time-dependent dipole and the dependence of the harmonic order on the ionization and emission times of H atom. Fig. 2 shows the time-frequency
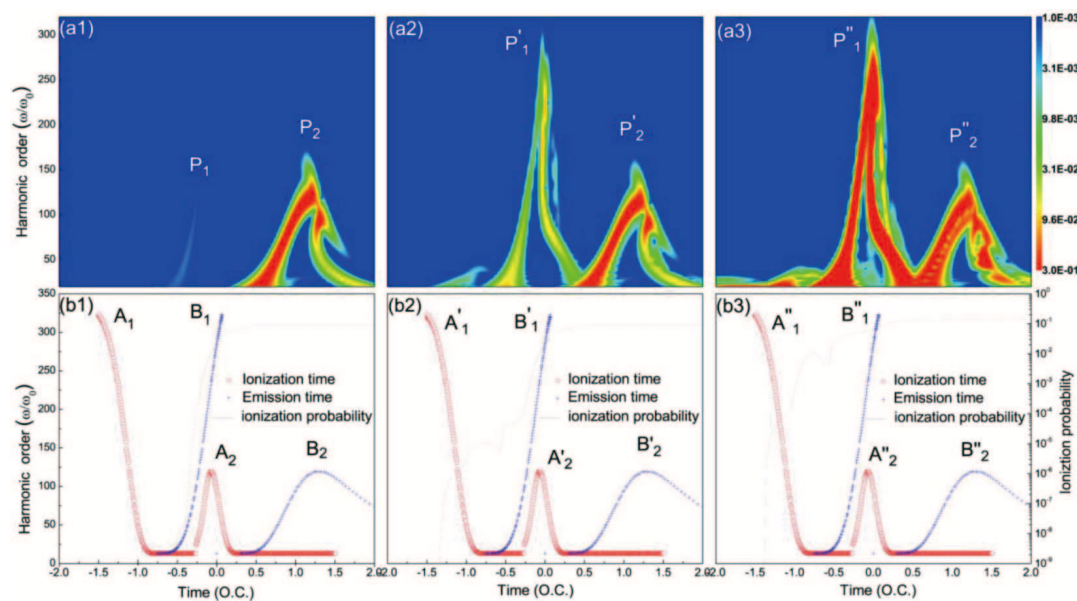
Figure 2: (Color online) Illustration of the time-frequency analysis ((a1)-(a3)) and the dependence of the harmonic order on the ionization (red circles) and emission times (blue asterisk) ((b1)-(b3)) for the chirped fundamental field only, the chirped fundamental field combined with a 256 nm UV field and chirped fundamental field combined with a 128 nm UV field (Corresponding to HHG of Fig.1(b)), respectively. The black dotted curve presents the corresponding ionization probability.

distribution of HHG (Figs. 2(a1)-(a3)), corresponding three-step model and ionization probability (Figs. 2(b1)-(b3)) in the chirped field only, a chirped fundamental field combined with a 256 nm UV pulse and a chirped fundamental field combined with a 128 nm UV pulse, respectively. In Fig. 2(a1), there are two peaks marked P_1 and P_2, the intensity of the peak P_2 is stronger than that of the peak P_1, the maximum harmonic order of P_2 is about $120\omega_0$. It is apparently seen that the long trajectory is suppressed and the short trajectory is relatively enhanced. In Fig. 2(a2), there are two peaks marked P'_1 and P'_2. We can see that after adding a 256 nm UV pulse on the chirped fundamental field, the harmonic emission after -0.5 O.C. is greatly enhanced. The maximum harmonic order of P'_1 and P'_2 are about $260\omega_0$ and $120\omega_0$, which can well explain the double-plateau structure of the harmonic spectrum (red solid curve) in Fig. 1(b). When we use a 128 nm UV pulse instead of the 256 nm UV pulse (as shown in Fig. 2(a3)), which also has two peaks marked P''_1 and P''_2. The intensity of the peak P''_1 is stronger than that of the peak P'_1, which means the intensity of harmonics can be greatly enhanced, which is consistent with the result in Fig. 1(b).

In Fig. 2(b1), there are two main peaks of kinetic energy as a function of ionization times, marked as A_1 and A_2 and two main peaks of kinetic energy as a function of emission times, marked as B_1 and B_2 in the chirped field only case. We can see that the electron ionized from -1.5 O.C. to -1.0 O.C. is returned from -0.5 O.C. to 0.0 O.C., while the electron ionized from -0.5 O.C. to 0.2 O.C. is returned from 0.5 O.C. to 1.25 O.C., the maximum
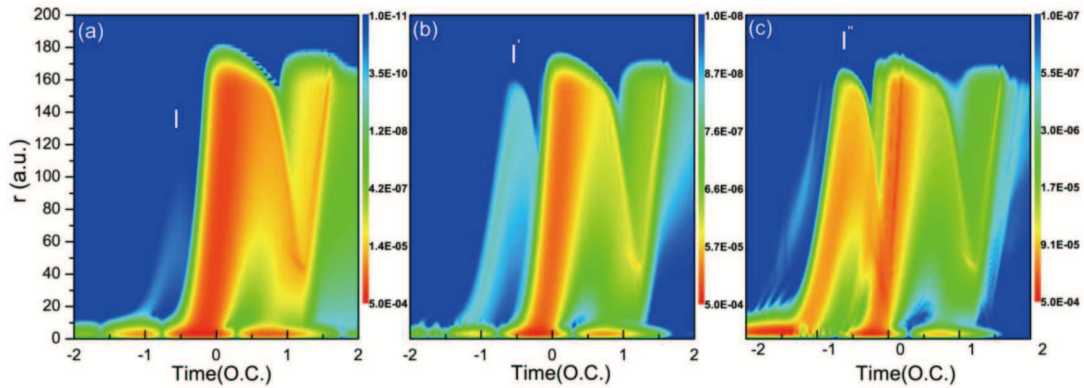
Figure 3: (Color online) Contour plot of the time evolution of a detailed view of the electronic probability density $G(r,t)$ in a chirped field only, a chirped fundamental field combined with a 256 nm UV pulse and a chirped fundamental field combined with a 128 nm UV pulse, respectively.

harmonic order of B_1 is about $260\omega_0$, the maximum harmonic order of B_2 is about $120\omega_0$. The ionization probability before -0.5 O.C. is very low (see the black dotted curve in Fig. 2(b1)), which causes lower harmonic efficiency. Thus, the peak B_1 can be ignored, only the peak B_2 is left to contribute to HHG, which is consistent with the result in Fig. 2(a1). In Fig. 2(b2), the ionization probability increases rapidly near -1.5 O.C. when the 256 nm UV pulse is added. In the following discussion, we will explain why a broadband and highly enhanced supercontinuum HHG spectra (red solid curve in Fig. 1(b)) can be generated.

When a 256 nm UV pulse is added, first, the ionization occurs earlier at about -1.5 O.C. and the ionization probability is enhanced by about three orders of magnitude compared to that of chirped field only case (see the black dotted curve in Fig. 2(b2)). Thus, the two emission peaks B'_1, B'_2 and the corresponding ionization peaks A'_1, A'_2 are all contributed to the HHG; Second, only the short trajectory of the peak B'_1 is left to contribute to the HHG for the harmonic from 120th to 260th order. Thus a single quantum path control is realized, which is advantageous to produce an isolated attosecond pulse. When we use a 128 nm UV pulse instead of the 256 nm UV pulse, as shown in Fig. 2(b3), the ionization probability is enhanced compared with that of the chirped fundamental field combined with a 256 nm UV pulse case, which is consistent with the result in Figs. 2((a2) and (a3)) and Fig. 1(b).

Furthermore, the time evolution of the electronic probability density $P(r,t)$ is also illustrated to clarify this physical mechanism. From Fig. 3(a), we can see the intensity of the peak I is weaker, which means the electronic probability density at T $\leq$ -0.5 O.C. is very low, most of electrons are bounded around the nucleus in the chirped field only. The electronic probability density begins to increase rapidly at around T = -0.5 O.C., then the laser field reverses its direction, some of the electrons moving towards the nuclei undergo a forward scattering from 0.5 O.C. to 1.25 o.c and emit an energetic photon, which is consistent with the result in Fig. 1(a) and Fig. 2(a1). As shown in Fig. 3(b), when

the 256nm UV pulse is added, the intensity of the peak I′ is much stronger than that of the peak I, which means the electronic probability density begins to increase rapidly at about -1.5 O.C., the electrons moves farther and gain higher kinetic energy in the continuum and emits more energetic photons from -0.5 O.C. to 0.2 O.C.. In Fig. 3(c), when the 128 nm UV pulse is added, compared with 256 nm UV pulse case, much more electron ionizes from -1.75 O.C. and most of electrons come back at around 0.5 O.C., accordingly, the intensity of the peak I″ is much stronger than that of the peak I′, which is in agreement with Figs. 2(a2), (a3), (b2) and (b3).

In Fig. 4, a 88 as and a 64 as pulse can be generated by superposing the HHG from
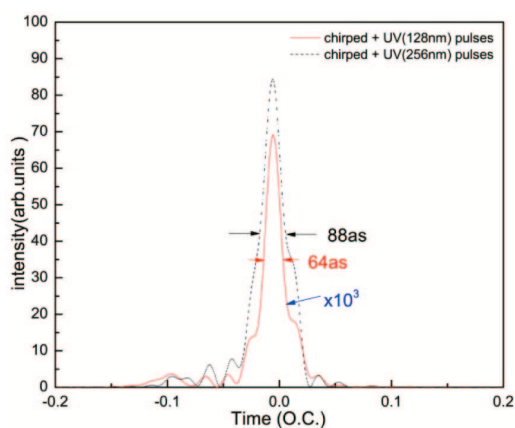

Figure 4: (Color online) Temporal profiles of the attosecond pulses generated from H atom by superposing the harmonics from 200th to 260th order in a chirped fundamental field combined with a 256nm UV pulse (black solid curve) and a chirped fundamental field combined with a 128 nm UV pulse (red dashed curve), respectively.
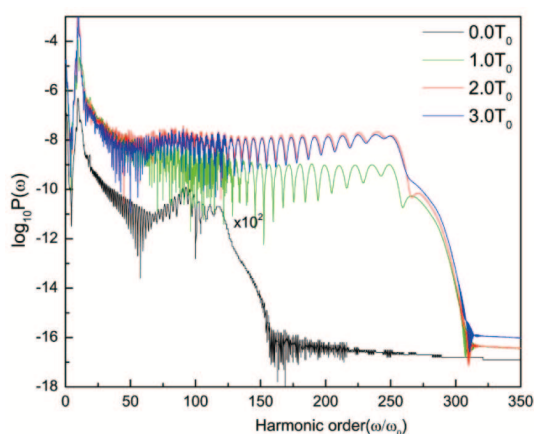

Figure 5: (Color online) The harmonic spectra with various time delays between the chirped fundamental field and a 128nm UV pulse, where black solid curve, green solid curve, red solid curve and blue solid curve presents the cases of $\tau = 0.0$ T$_0$, $\tau = 1.0$ T$_0$, $\tau = 2.0$ T$_0$ and $\tau = 3.0$ T$_0$, respectively.

the 200th to the 260th order harmonics in the chirped fundamental field combined with a 256 nm UV pulse and a chirped fundamental field combined with a 128nm UV pulse, respectively. The intensity of the 64 as pulse is three orders of magnitude higher than the 88 as pulse.

Finally, we investigate the influence of the HHG spectrum with four different delays between the chirped fundamental field and the 128 nm UV pulse in Fig. 5. We can see from Fig. 5 that the HHG spectrum has a cutoff of 120th order in the case $\tau = 0.0\ T_0$. When the time delay increases from $\tau = 1.0\ T_0$ to $\tau = 3.0\ T_0$, it can be apparently seen that the plateau is extended to about 260th order, the intensity of the HHG is enhanced from $\tau = 1.0\ T_0$ to $\tau = 2.0\ T_0$. For the case of $\tau = 3.0\ T_0$, the intensity of the HHG is quite similar to that in the case $\tau = 2.0\ T_0$. The result shows that time delay has great influence on HHG process. On the other hand, the electrons can make transitions from ground state to excited state in its best after $\tau = 2.0\ T_0$.

4   Conclusions

In conclusion, we have theoretically investigated the HHG and the attosecond pulse generation of H atom in the chirped fundamental field combined with a UV pulse by solving the time-dependent Schrödinger equation (TDSE) accurately with time-dependent generalized pseudospectral (TDGPS) method. The result shows that when a 256 nm UV pulse is added, its photon energy of $E_{256nm} = 5.15$ eV is close to that of the two-photon transition between the ground and excited states of the H atom, the harmonic spectrum presents a double-plateau structure with two cutoffs of the 120th order and the 260th order, the intensity of the second plateau is about six orders higher than that of chirped field only case. When we choose a 128 nm UV pulse instead, its photon energy of $E_{128nm} = 10.3$ eV is close to that of the one-photon transition between the ground and excited states of the H atom, the second plateau is about three orders of magnitude higher than that of combined 256 nm UV pulse case, the two plateaus merge into one plateau and a broadband supercontinuum can be achieved. We also investigate the corresponding HHG from H atom initially prepared in the 1st excited state in the chirped fundamental field only, the HHG is quite similar to that initially prepared in the ground state in the combination of a chirped fundamental field and a 128 nm UV pulse case. The HHG process can be illustrated by the semi-classical three-step model and the time-frequency analysis. In addition, the ionization probability and electron wavepacket as functions of time are also calculated to further illustrate this phenomenon. Furthermore, we also discuss the influence of time delay between the chirped fundamental field and the 128nm UV pulse on HHG process. Finally, by superposing the harmonics in the range of 200th-260th order, an isolated attosecond pulse with a duration of about 64 as can be generated.

References

[1] Popmintchev T. *et al.*; Science. 2012, 336, 1287-1291.

[2] Heslar J.; Telnov D.; Chu Shih-I.; Phys. Rev. A. 2011, 83, 043414(1-7).

[3] Corkum P. B.; Krausz F.; Nat. Phys. 2007, 3, 381-387.

[4] Li L. Q.; Xu Y. Y.; Miao X. Y.; J. At. Mol. Sci. 2016, 7, 1-10.

[5] Spielmann Ch.; Burnett N. H.; Sartania S.; Koppitsch R.; Schn?rer M.; Kan C.; Lenzner M.; Wobrauschek P.; Krausz F.; Science. 1997, 278, 661-664.

[6] Xia C. L.; Miao X. Y.; J. At. Mol. Sci. 2016, 7, 17-24.

[7] Corkum P. B.; Phys. Rev. Lett. 1993, 71, 1994-1997.

[8] Krause J. L.; Schafer K. J.; Kulander K. C.; Phys. Rev. Lett. 1992, 68, 3535-3538.

[9] Schafer K. J.; Yang B.; DiMauro L. F.; Kulander K. C.; Phys. Rev. Lett. 1993, 70, 1599-1602.

[10] Ge X. L.; Wang T.; Guo J. and Liu X. S.; Phys. Rev. A. 2014, 89, 023424(1-6).

[11] Zhang G. T.; Bai T. T.; Zhang M. G.; J. At. Mol. Sci. 2013, 4, 251-260.

[12] Jiao Z. H.; Wang G. L.; Li P. C; Zhou X. X.; Phys. Rev. A. 2014, 90, 025401(1-4).

[13] Zhang K.; Chen J.; Hao X. L.; Fu P. M.; Yan Z. C.; Wang B. B.; Phys. Rev. A. 2013, 88, 043435(1-5).

[14] Aközbek N.; Iwasaki A.; Becker A.; Scalora M.; Chin S. L.; Bowden C. M.; Phys. Rev. A. 2002, 89, 143901(1-4).

[15] Mauritsson J.; Johnsson P.; Gustafsson E.; L'Huillier A.; Schafer K. J.; Gaarde M. B.; Phys. Rev. Lett. 2006, 97, 013001(1-4).

[16] Yuan K. J.; Bandrauk A. D.; Phys. Rev. Lett. 2013, 110, 023003(1-5).

[17] Ge X. L.; Du H.; Guo J.; Liu X. S.; Opt. Express. 2015, 23, 008837-008844.

[18] Miao X. Y.; Liu S. S.; Chin. Phys. Lett. 2015, 32, 013301(1-5).

[19] Xia C. L.; Zhang G. T.; Wu J.; Liu X. S.; Phys. Rev. A. 2010, 81, 043420(1-6).

[20] Jin C.; Le A. T.; Trallero-Herrero C. A.; Lin C. D.; Phy. Rev. A. 2011, 84, 043411(1-12).

[21] Liu C. D.; Li R. X.; Zeng Z. N.; Zheng Y. H.; Liu P.; Xu Z. Z.; Optics Letters. 2010, 35, 2618-2620.

[22] Ciappina M. F.; Biegert J.; Quidant R.; Lewenstein M.; Phys. Rev. A. 2012, 85, 033828(1-11).

[23] He L. X.; Wang Z.; Li Y.; Zhang Q. B.; Lan P. F.; Lu P. X.; Phys. Rev. A. 2013, 88, 053404(1-7).

[24] Cao X.; Jiang S. C.; Yu C.; Wang Y. H; Bai L. H.; Lu R. F.; Opt. Express. 2014, 22, 026153-026161.

[25] Wu J.; Zhai Z.; Liu X. S.; Chin. Phys. B. 2010, 19, 093201(1-4).

[26] Carrera J. J.; Chu S. I.; Phys. Rev. A. 2007, 75, 033807(1-5).

[27] Zhai Z.; Yu R. F.; Liu X. S.; Y. J. Yang; Phys. Rev. A. 2008, 78, 041402(1-4).

[28] Mohebbi M.; Phys. Rev. A. 2015, 91, 023835(1-11).

[29] Ishikawa K.; Phys Rev Lett. 2003, 91, 043002(1-4).

[30] Chen Y. J.; Liu J.; Hu B. B.; Phys. Rev. A. 2009, 79, 033405(1-5).

[31] Yavuz I.; Altun Z.; Topcu T.; J. Phys B: At. Mol. Opt. Phys. 2011, 44, 135403-135411.

[32] Wirth A.; Hassan M. Th.; Grguraš I.; Gagnon J.; Moulet A.; Luu T. T.; Pabst S.; Santra R.; Alahmed Z. A.; Azzeer A. M.; Yakovlev V. S.; Pervak V.; Krausz F.; Goulielmakis E.; Science. 2011, 334, 195-200.

[33] Bandrauk A. D.; Chelkowski S.; Shon N. H.; Phys. Rev. Lett. 2002, 89, 283903(1-4).

[34] Johnsson P.; López-Martens R.; Kazamias S.; Mauritsson J.; Valentin C.; Remetter T.; VarjúK.; Gaarde M. B.; Mairesse Y.; Wabnitz H.; Salières P.; Balcou Ph.; Schafer K. J.; L'Huillier A.; Phys. Rev. Lett. 2005, 95, 013001(1-4).

[35] K. J. Schafer; M. B. Gaarde; A. Heinrich; J. Biegert; and U. Keller; Phys. Rev. Lett. 92 (2004)

023003.

[36] Lan P. F.; Lu P. X.; Cao W.; Wang X. L.; Phys. Rev. A. 2007, 76, 043808(1-5).

[37] Hong W. Y.; Li Y. H.; Lu P. X.; Lan P. F.; Zhang Q. B.; Wang X. B.; J. Opt. Soc. Am. B. 2008, 25, 1684-1689.

[38] Li P. C.; Zhou X. X.; Wang G. L.; Zhao Z. X.; Phy. Rev. A. 2009, 80, 053825(1-7).

[39] Feng L. Q.; Li W. I.; Liu H.; Yuan M. H.; Yuan S. P.; Chu T. S.; Spectroscopy Letters. 2014, 47, 781-789.

[40] Tong X. M.; S. I. Chu; Chem. Phys. 1997, 217, 119-130.

[41] Li P. C.; Laughlin C.; Chu S. I.; Phys. Rev. A. 2014, 89, 023431(1-5).